



УДК 621.762; 62-408.2

<https://doi.org/10.17073/1997-308X-2023-4-51-58>

Научная статья

Research article



Электроискровое осаждение покрытий Fe–Cr–Cu на сталь Ст3

А. А. Бурков[✉], М. А. Кулик

Институт материаловедения Хабаровского федерального исследовательского центра

Дальневосточного отделения РАН

Россия, 680042, г. Хабаровск, ул. Тихоокеанская, 153

[✉ burkovalex@mail.ru](mailto:burkovalex@mail.ru)

Аннотация. Известно, что хром в составе металлических композиций формирует плотные пассивирующие пленки, замедляющие коррозию. Новое Fe–Cr–Cu-покрытие осаждено на сталь Ст3 электроискровой обработкой в анодной смеси, состоящей из медных и титановых гранул с добавлением порошка хрома в количестве от 4,85 до 13,26 мас. %. Привес катода увеличивался почти вдвое с ростом добавки порошка хрома в анодную смесь. Структуру покрытий исследовали методами рентгенофазового анализа, сканирующей электронной микроскопии и энергодисперсионной спектроскопии. Фазовый состав покрытий представлен феррохромом и медью. Показано, что предложенная методика электроискровой обработки позволяет получать Fe–Cr–Cu-покрытия со средней концентрацией хрома от 55 до 83 ат. %. Среднее содержание меди в приготовленных покрытиях находилось в диапазоне от 5 до 16 ат. %. Наибольшая концентрация хрома наблюдалась в покрытии, приготовленном с добавкой 13,26 мас. % Cr в анодную смесь. Коррозионное поведение покрытий исследовали методами потенциодинамической поляризации и импедансной спектроскопии в 3,5 %-ном растворе NaCl. Поляризационные испытания показали, что нанесение Fe–Cr–Cu-покрытий на сталь Ст3 позволяет повысить ее коррозионный потенциал от 12 до 19 % и снизить ток коррозии от 1,5 до 3,4 раза. Микротвердость поверхности покрытий составляла от 3,08 до 4,37 ГПа, а коэффициент трения – от 0,75 до 0,91. Максимальная твердость и наименьший коэффициент трения наблюдались у покрытия с наибольшим содержанием хрома. Показано, что Fe–Cr–Cu-покрытия позволяют улучшить износостойкость поверхности стали Ст3 от 1,5 до 3,8 раз.

Ключевые слова: покрытия Fe–Cr–Cu, электроискровое легирование, сталь Ст3, плотность тока коррозии, коэффициент трения, твердость, износ

Благодарности: Работа выполнена в рамках государственного задания Министерства науки и высшего образования Российской Федерации № 075-01108-23-02 (тема № 123020700174-7 «Создание и исследование новых металлических, керамических, интерметаллидных, композиционных материалов и наноструктурных покрытий с высокими физико-химическими и эксплуатационными свойствами»).

Для цитирования: Бурков А.А., Кулик М.А. Электроискровое осаждение покрытий Fe–Cr–Cu на сталь Ст3. *Известия вузов. Порошковая металлургия и функциональные покрытия*. 2023;17(4):51–58. <https://doi.org/10.17073/1997-308X-2023-4-51-58>

Electrospark deposition of Fe–Cr–Cu coatings on St3 steel

A. A. Burkov[✉], M. A. KulikInstitute of Materials Science of the Khabarovsk Federal Research Center
of the Far Eastern Branch of the Russian Academy of Sciences

153 Tikhookeanskaya Str., Khabarovsk 680042, Russia

[✉ burkovalex@mail.ru](mailto:burkovalex@mail.ru)

Abstract. It is well-known that chromium in metallic compositions forms dense passivating films that slow down corrosion. The new Fe–Cr–Cu coating was applied on St3 steel through electrospark deposition in an anode mixture consisting of copper and titanium granules, with the addition of chromium powder ranging from 4.85 to 13.26 wt. %. The weight gain of the cathode increased

nearly twofold with the addition of chromium powder to the anode mixture. The structure of the coatings was analyzed through X-ray phase analysis, scanning electron microscopy, and energy dispersive spectrometry. The phase composition of the coatings consists of ferrochrome and copper. It is demonstrated that the proposed method of electrospark processing allows for the creation of Fe–Cr–Cu coatings with an average chromium concentration ranging from 55 to 83 at. %. The average copper content in the prepared coatings varied from 5 to 16 at. %. The highest concentration of chromium was observed in the coating prepared with the addition of 13.26 wt. % Cr to the anodic mixture. The corrosion behavior of the coatings was investigated using potentiodynamic polarization and impedance spectroscopy in a 3.5 % NaCl solution. Polarization tests have shown that applying Fe–Cr–Cu coatings to St3 steel can increase its corrosion potential by 12 to 19 % and reduce the corrosion current by 1.5 to 3.4 times. The microhardness of the coating surface ranged from 3.08 to 4.37 GPa, and the coefficient of friction ranged from 0.75 to 0.91. The maximum hardness and the lowest coefficient of friction were observed in the coating with the highest chromium content. It has been demonstrated that Fe–Cr–Cu coatings can enhance the wear resistance of the surface of St3 steel by 1.5 to 3.8 times.

Keywords: Fe–Cr–Cu coatings, electrospark deposition, St3 steel, corrosion current density, coefficient of friction, hardness, wear

Acknowledgements: This research has received support from the Ministry of Science and Higher Education of the Russian Federation, Governmental contract No. 075-01108-23-02 “Development and study of innovative metallic, ceramic, intermetallic, composite materials and nanostructural coatings with superior physicochemical and operational properties”).

For citation: Burkov A.A., Kulik M.A. Electrospark deposition of Fe–Cr–Cu coatings on St3 steel. *Powder Metallurgy and Functional Coatings*. 2023;17(4):51–58. <https://doi.org/10.17073/1997-308X-2023-4-51-58>

Introduction

The economic damage caused by corrosion is estimated at approximately US\$ 2.5 trillion, which is equivalent to 3.4 % of the world’s gross domestic product [1]. This figure does not include indirect losses associated with negative environmental impacts and the potential for emergency incidents [2]. As of 2014, China’s total spending on anti-corrosion measures reached US\$ 152 billion, with the majority allocated to coatings (66.15 %) and surface treatment (13.24 %) [3]. In the Russian Federation, the annual loss of metals due to corrosion amounts to up to 12 % of the total mass of the metal stock, which corresponds to a loss of up to 30 % of the metal produced annually [4; 5].

It is well-known that the corrosion resistance of steels can be significantly improved by applying protective coatings [6]. Currently, the most widely used methods involve electroplating with chromium or nickel-chromium compositions. However, electroplated coatings exhibit poor adhesion and are susceptible to damage under harsh operating conditions, often resulting in local peeling of the chromium coating at the interface with the substrate [7]. Moreover, hexavalent chromium, which is used in electroplating, is classified as a hazardous substance. Air pollution from hexavalent chromium can lead to fatal diseases among plant employees, and severe wastewater contamination poses environmental risks, prompting several governments to restrict the use of electroplating [8].

Widespread magnetron sputtering methods are not well-suited for use with ferromagnetic materials due to poor plasma stability. In contrast to electroplating, electrospark deposition (ESD) offers superior adhesion of coatings because of the metallurgical bonding between the deposited material and the substrate. Chromium is commonly used to coat steels because it

forms a passive Cr_2O_3 oxide on its surface, contributing to corrosion resistance [9; 10]. Moreover, Cr–Ti composite coatings show higher corrosion resistance compared to pure chromium or titanium coatings [11]. Furthermore, Cr–Ti composite coatings exhibit enhanced corrosion resistance when compared to pure chromium or titanium coatings [11]. However, it is known that even corrosion-resistant chromium alloys can experience localized corrosion due to bacteria-induced ennoblement [12]. On the other hand, the addition of more than 5 wt. % Cu to the alloy has been found to confer sustained antibacterial properties [13]. Consequently, adding copper to the Cr–Ti composite should provide it with antimicrobial capabilities and reduce the risk of corrosion caused by microbially induced ennoblement. Previously, we developed an automated ESD technique using a nonlocalized electrode, potentially matching the performance and energy efficiency of chromium plating [14; 15].

The objective of this study was to assess the suitability of ESD with a nonlocalized electrode for applying protective Fe–Cr–Cu coatings to St3 steel. Additionally, we aimed to investigate the impact of the concentration of chromium powder in the anode mixture on the structure, corrosion resistance, and tribological characteristics of the coatings.

Experimental

Copper and titanium granules were used in a molar ratio of 3:2 ($\text{Cu}_{60}\text{Ti}_{40}$) along with chromium powder with a purity of 98.5%, as the anode mixture. $\text{Cu}_{60}\text{Ti}_{40}$ granules was chosen as the sources of copper and titanium. These granules were created by cutting copper (M0) and titanium (VT-00) wires with a 4 mm diameter into pieces that were 4 ± 0.5 mm long. The chromium powder was pre-ground using a Retsch PM400 plane-

tary mill (Retsch GmbH, Germany) in alcohol and an argon atmosphere at a speed of 250 min^{-1} for 80 min. The average size of chromium particles after grinding was $1.90 \pm 0.98 \text{ }\mu\text{m}$. The amount of chromium added to the anode mixture varied from 4.85 to 13.26 wt. % (Table 1). The substrate (cathode) was made of St3 steel in the shape of a cylinder with a diameter of 12 mm and a height of 10 mm. The facility for depositing coatings using a nonlocalized anode with the addition of Cr_3C_2 powder is described in detail in [16]. The IMES-40 discharge pulse generator (Institute of Materials Science, Khabarovsk) generated rectangular current pulses with an amplitude of 110 A, 100 μs , 1000 Hz, and 40 V. To prevent oxidation of the sample surfaces, argon was supplied to the working volume of the container at a rate of 5 l/min.

The kinetics of mass transfer were studied by alternately weighing the cathode every 2 min using ESA on a Vibra HT120 analytical balance (Shinko Denshi, Japan) with an accuracy of 0.1 mg. The total processing time for one sample was 8 min. To ensure reproducibility of the results, the cathode weight gain was studied for three samples from each series.

The phase composition of the prepared coatings was analyzed using a DRON-7 X-ray diffractometer (NPP “Burevestnik”, St. Petersburg) with CuK_α radiation in the angle range $2\theta = 20^\circ\text{--}90^\circ$. The microstructure of the coatings was examined using a Vega 3 LMH scanning electron microscope (SEM) (Tescan, Czech Republic) equipped with an X-max 80 energy dispersive spectrometer (EDS) (Oxford Instruments, UK).

The roughness of the coatings was measured using a TR 200 profilometer (TIME GROUP Inc., China).

Polarization tests were conducted in a three-electrode cell using a 3.5 % NaCl solution. A P-2X galvanostat (Electro Chemical Instruments, Chernogolovka) with a scanning speed of 4 mV/s was employed. A standard silver chloride electrode served as the reference electrode, and a paired platinum electrode ETP-02 was utilized as the counter electrode. Before recording, the samples were allowed to stabilize in the open circuit current for 30 min. The corrosion current density was determined from the plots using the Tafel extrapolation method.

Impedance studies were carried out using a Z2000 device (Elins LLC, Moscow) within a frequency range of 100,000 to 1 Hz.

The hardness of the coatings was measured using a PMT-3M microhardness tester (JSC LOMO, St. Petersburg) with a load of 0.5 N, employing the Vickers method. The wear resistance and coefficient of friction of the samples were assessed following the ASTM G99-17 procedure, involving dry sliding friction at a speed of 0.47 m/s under a load of 25 N. The testing time was set at 10 min, and high-speed steel M45 disks with a hardness of 60 HRC were employed as the counterbodies. Wear was evaluated gravimetrically, with each sample type subjected to at least three times.

Results and discussion

As the electrospark treatment time increased, the St3 steel cathode continuously gained weight, and the rate of weight gain significantly increased with the content of chromium powder in the anode mixture ranging from 4.85 to 9.25 wt. % (Fig. 1, *a*). With a larger quantity of Cr powder (from 9.25 to 13.26 wt. %), the weight gain of the substrates increased slightly, considering the margin of error. This observation suggests that the chromium powder content in the anode mixture is approaching an optimal value. In general, the cathode weight gain indicates that chromium powder can be successfully deposited on St3 steel using the ESD method with a $\text{Cu}_{60}\text{Ti}_{40}$ anode mixture.

X-ray diffraction patterns of the prepared coatings are displayed in Fig. 1, *b*. Reflections of ferrochrome Fe–Cr (#34–396 PDWin base) and copper (#4–836) are evident in the X-ray spectra of the coatings. Based on the intensities of the reflections, it is evident that the composition of the coatings was predominantly ferrochrome, which is a solid solution of chromium substituting for iron. This finding aligns with data from [17], where M50 steel was treated with the ESD method using a chromium electrode. The relative intensity of copper reflections in the X-ray spectra decreased with an increasing addition of chromium to the anode mixture, indicating a reduction in the copper concentration within the coatings.

The average thickness of the coatings increased within the range of 38.1 to 48.6 μm with an increasing addition of chromium to the anode mixture (Table 2). Figure 2, *a* displays an electron image of the cross-section of the Cr5 coating in the back-reflected electron mode. Within the coating's microstructure, there are light inclusions rich in copper (Fig. 2, *b*). These inclusions are likely the ones identified in the X-ray diffraction pattern. The coating exhibits a dense structure with a minimal number of small pores and inclusions

Table 1. The composition of the anode mixture and the designation of coatings

Таблица 1. Состав анодной смеси и обозначение покрытий

Designation	Ratio of metallic granules, at. %		Powdered chrome, wt. %
	Cu	Ti	
Cr5	60	40	4.85
Cr9			9.25
Cr13			13.26

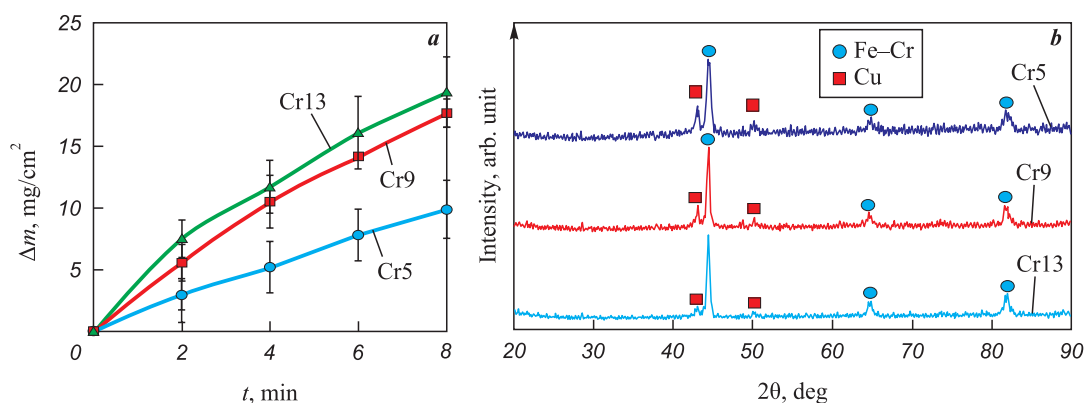


Fig. 1. The kinetics of cathode weight gain during the electrospark deposition of coatings (a) and X-ray diffraction patterns of the deposited coatings (b)

Рис. 1. Кинетика привеса катода при электроискровом нанесении покрытий (a) и рентгеновские дифрактограммы осажденных покрытий (b)

of copper oxides. The presence of copper oxides is a result of copper's high affinity for oxygen, even with the supply of argon to the container containing the granules. A significant accumulation of copper was found at the interface between the coating and the substrate (as shown in Fig. 2, c). This accumulation likely formed when a discharge occurred between the substrate and the copper granule at the outset of the ESD process.

The average chromium concentration in the coating composition ranged from 55 to 83 at. %. As the chromium content in the anodic mixture increased, its concentration in the coating exhibited a non-monotonic trend, with a minimum for the Cr9 sample and a maximum for the Cr13 sample (Fig. 3). Consequently, the average copper concentration in the coatings decreased from 16 to 5 at. %, reaching its maximum in the Cr9 sample.

The discrepancy between the data from X-ray phase analysis and energy dispersive analysis regarding the trend of changes in copper content with the addition of chromium to the anode mixture can be attributed to the fact that the concentration of chromium in the ferrochrome phase can vary widely. Additionally, the results obtained through the EDS method are generally considered more accurate compared to X-ray phase analysis. The average titanium content in the coatings ranged from 0.6 to 4 at. %. A comparison of copper and titanium data reveals that copper from the granules is

Table 2. Characteristics of coatings

Таблица 2. Характеристики покрытий

Sample	Thickness, μm	Roughness R_a , μm	Microhardness, GPa
Cr5	38.1 ± 12.2	3.82 ± 0.79	3.46 ± 0.44
Cr9	47.9 ± 6.0	4.63 ± 0.85	3.08 ± 0.26
Cr13	48.6 ± 5.4	4.04 ± 1.24	4.37 ± 0.46

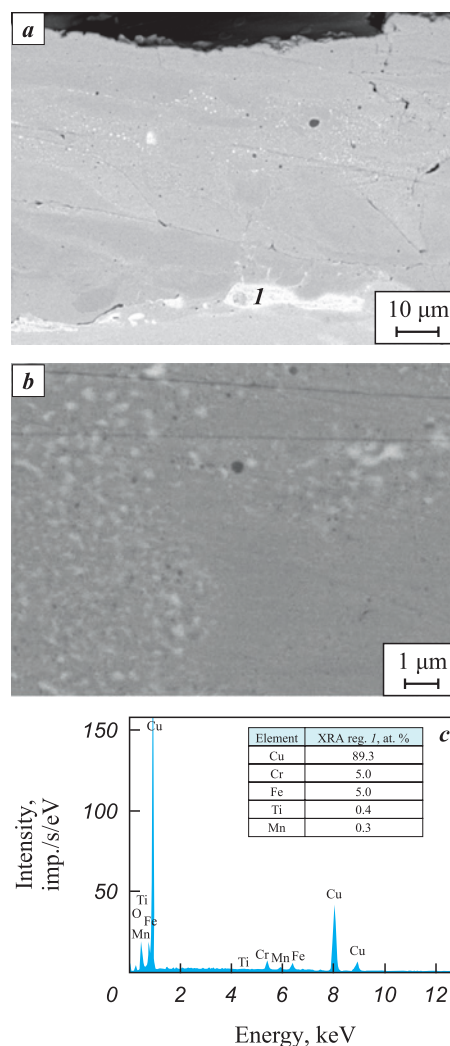


Fig. 2. The SEM images of the Cr5 coating sample cross-section (a), its microstructure (b), and the EDS spectrum of a light inclusion (c)

Рис. 2. СЭМ-изображения поперечного сечения покрытия Cr5 (a), его микроструктура (b) и ЭДС-спектр светлого включения (c)

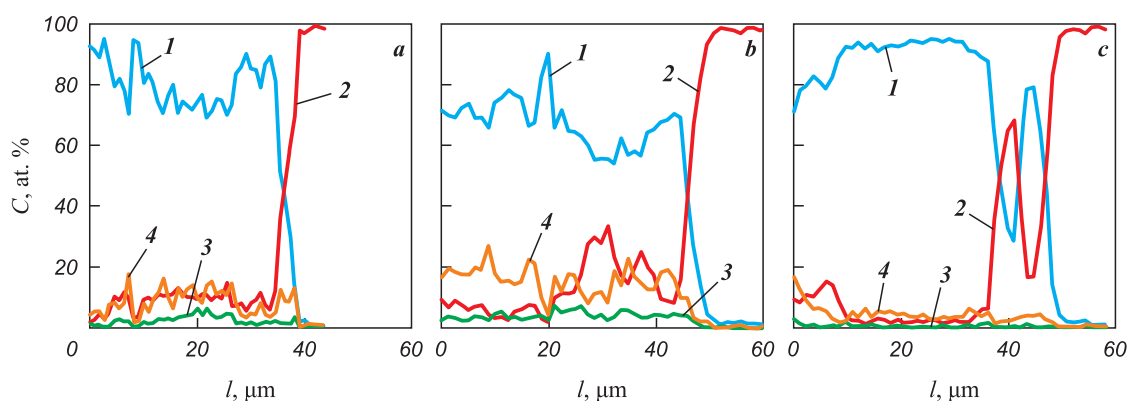


Fig. 3. The EDS analysis of elemental distribution along the coating cross-sections of samples Cr5 (*a*), Cr9 (*b*), and Cr13 (*c*)
1 – Cr, 2 – Fe, 3 – Ti, 4 – Cu

Рис. 3. Типичное распределение элементов по поперечному сечению покрытий Cr5 (*a*), Cr9 (*b*), Cr13 (*c*) согласно ЭДС-анализу
1 – Cr, 2 – Fe, 3 – Ti, 4 – Cu

much more actively transferred into the coating during ESD than titanium. This can be attributed to the higher melting point of titanium (1660 °C) when compared to copper (1083 °C).

An increase in the corrosion potential of St3 steel after coating indicates a reduction in its susceptibility to spontaneous corrosion (Fig. 4, *a*). To provide a detailed description of the corrosion behavior of the samples, the corrosion current density I_{corr} was calculated. The values of I_{corr} are in the range from 43.7 to 101.1 A/cm², as shown in Table 3. The corrosion current density varied inversely with the chromium concentration in the coatings, with a minimum for the Cr9 sample and a maximum for the Cr13 sample,

mirroring the trend observed in the corrosion potential. The corrosion current density of the coatings was 1.47 to 3.39 times lower than that of St3 steel, despite the coatings' higher actual metal-to-electrolyte interface formed by the roughness of the coatings (see Table 2) in comparison to steel.

The electrical impedance spectra in a 3.5 % NaCl solution at room temperature are presented in Fig. 4, *b*. In this representation, the Im and Re axes represent the imaginary and real components of electrical impedance, respectively. The Nyquist diagrams for all coatings feature similar semicircular capacitive contours in the high-frequency region. Typically, a larger radius of the capacitive arc indicates higher corrosion resis-

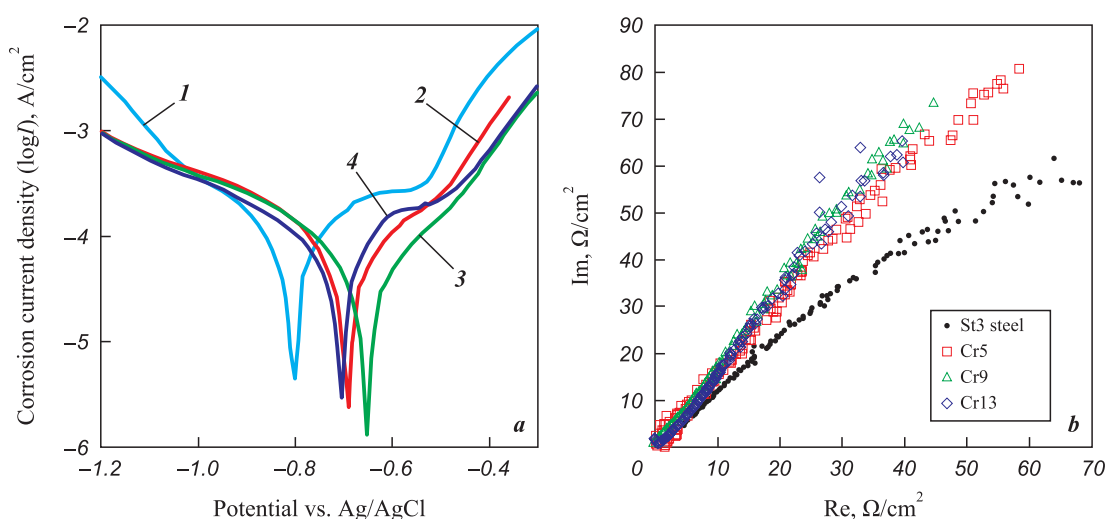


Fig. 4. The potentiodynamic polarization curves (*a*) and Nyquist plot (*b*) of Fe–Cr–Cu coatings and St3 steel
1 – steel St3, 2 – Cr5, 3 – Cr9, 4 – Cr13

Рис. 4. Потенциодинамические поляризационные кривые (*a*) и импедансные графики в координатах Найквиста (*b*) Fe–Cr–Cu-покрытий и стали Ст3
1 – сталь Ст3, 2 – Cr5, 3 – Cr9, 4 – Cr13

Table 3. Corrosion potential and corrosion current density of coatings

Таблица 3. Коррозионный потенциал и ток коррозии покрытий

Sample	$E_{\text{corr}}, \text{V}$	$I_{\text{corr}}, \mu\text{A}/\text{cm}^2$
St3	–0.80	148.3
Cr5	–0.69	64.9
Cr9	–0.65	43.7
Cr13	–0.70	101.1

tance of the material [18]. The radius of the capacitive circuit for all coatings was relatively close, but there was a tendency for it to increase with the addition of more chromium to the anode mixture. This implies that the corrosion resistance of Fe–Cr–Cu coatings improved with higher chromium concentrations. The radius of the capacitive circuit for St3 steel was notably smaller than that of the coatings, aligning with the potentiodynamic polarization data.

The microhardness measured at the surface of the coatings was consistent among all samples, ranging from 3.08 to 4.37 GPa (as shown in Table 2). As it is well-known, the microhardness of a coating is influenced by the phase composition and the distribution of residual stresses [19]. Chromium is known for its greater hardness compared to iron or copper. Consequently, the Cr9 coating with a low chromium concentration exhibited the lowest hardness, while the Cr13 coating with the highest chromium content displayed the highest hardness (see Fig. 3). Additionally, the increased hardness of the coatings was influenced by the refinement of the structure due to high cooling rates of the material after the ESD discharge completion [20]. Given that the hardness of St3 steel was 1.09 ± 0.2 GPa, the electrospark deposition of chromium can enhance the surface hardness by up to four times.

The average values of the coefficient of friction (COF) for the coatings ranged from 0.75 to 0.91 (Fig. 5, *a*). These higher COF values are in line with data from Fe–Cr coatings prepared through induction surfacing, where $COF = 0.9$ [21]. The coefficient of friction for the coatings was higher than that of St3 steel ($COF = 0.63$). Despite the relatively elevated COF level, the wear rate of the Fe–Cr–Cu coatings was 1.5 to 3.8 times lower than that of uncoated steel (Fig. 5, *b*). With an increasing chromium concentration in the anodic mixture, the wear of the electrospark coatings steadily increased from $1.88 \cdot 10^{-5}$ to $4.61 \cdot 10^{-5} \text{ mm}^3/(\text{N} \cdot \text{m})$. This is likely due to the embrittlement of coatings as they become enriched with chromium, resulting in increased fluctuations in the friction force in the coefficient of friction curves for the Cr6 sample (Fig. 5, *a*).

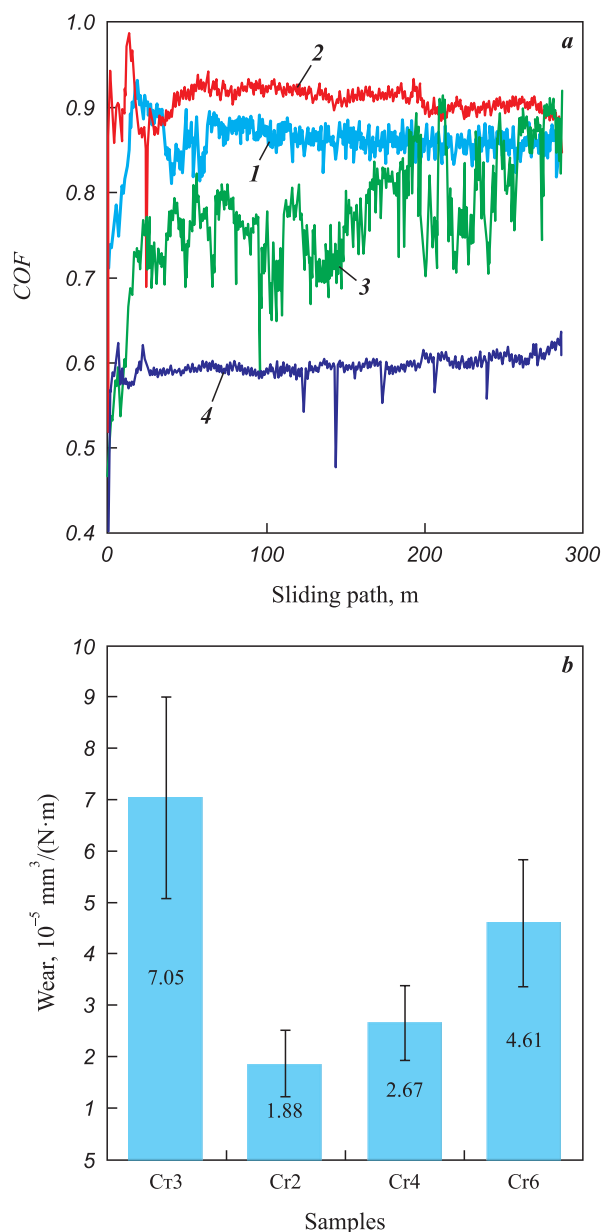


Fig. 5. The coefficient of friction (*a*) and wear (*b*) of coatings in comparison with St3 steel at a load of 25 N
1 – Cr2, 2 – Cr4, 3 – Cr6, 4 – steel St3

Рис. 5. Коэффициент трения (*a*) и износ (*b*) покрытий по сравнению со сталью Ст3 при нагрузке 25 Н
1 – Cr2, 2 – Cr4, 3 – Cr6, 4 – сталь Ст3

Conclusions

The method for depositing Fe–Cr–Cu coatings on St3 steel through electrospark treatment with a non-localized electrode in an anode mixture has been proposed. The anode mixture, consisting of copper and titanium granules supplemented with chromium powder ranging from 4.85 to 13.26 wt. %, allows for the production of coatings with chromium concentrations between 55 and 83 at. %. The coating with the highest chromium content was obtained when 13 wt. % of chromium was

added to the anode mixture. The average copper content in the coatings varied from 5 to 16 at. %. Polarization tests revealed that applying Fe–Cr–Cu coatings to St3 steel can increase its corrosion potential by 12 to 19 % and reduce the corrosion current by 1.5 to 3.4 times. The microhardness of the coating surface ranged from 3.08 to 4.37 GPa, while the coefficient of friction fell within the range of 0.75 to 0.91. The highest hardness and the lowest coefficient of friction were observed in the coating with the highest chromium content. It's worth noting that wear of the coatings increased with the addition of chromium powder to the anode mixture.

References / Список литературы

1. Lazorenko G., Kasprzhitskii A., Nazdracheva T. Anti-corrosion coatings for protection of steel railway structures exposed to atmospheric environments: A review. *Construction and Building Materials*. 2021;288:123115. <https://doi.org/10.1016/j.conbuildmat.2021.123115>
2. Kirchgeorg T., Weinberg I., Hörnig M., Baier R., Schmid M.J., Brockmeyer B. Emissions from corrosion protection systems of offshore wind farms: Evaluation of the potential impact on the marine environment. *Marine Pollution Bulletin*. 2018;136:257–268. <https://doi.org/10.1016/j.marpolbul.2018.08.058>
3. Hou B., Li X., Ma X., Cuiwei D., Zhang D., Zheng M., Xu W., Lu D., Ma F. The cost of corrosion in China. *npj Materials Degradation*. 2017;1(1):1–10. <https://doi.org/10.1038/s41529-017-0005-2>
4. Semenova I.V., Florianovich G.M., Khoroshilov A.V. Corrosion and corrosion protection. Moscow: Fizmatlit, 2002. 336 p. (In Russ.).
Семенова И.В., Флорианович Г.М., Хорошилов А.В. Коррозия и защита от коррозии. М.: Физматлит, 2002. 336 с.
5. Elizar'ev A.N., Aksenov S.G., Sarvarov T.M., Mikhailov S.A., Sinagatullin F.K., Elizar'eva E.N., Epimakhov N.L. Ensuring environmental and industrial safety at tank farms of oil refining enterprises. *International Research Journal*. 2022;117(3):32–37. (In Russ.).
Елизарьев А.Н., Аксенов С.Г., Сарваров Т.М., Михайлов С.А., Синагатуллин Ф.К., Елизарьева Е.Н., Эпимахов Н.Л. Обеспечение экологической и промышленной безопасности на резервуарных парках нефтеперерабатывающих предприятий. *Международный научно-исследовательский журнал*. 2022;117(3-1):32–37. <https://doi.org/10.23670/IRJ.2022.117.3.005>
6. Knyazeva Zh.V., Yudin P.E., Petrov S.S., Maksimuk A.V. Application of metallization coatings for protection of submersible electric motors of pumping equipment from influence of complicating factors in oil wells. *Powder Metallurgy and Functional Coatings*. 2020;(1):75–86. (In Russ.). <https://doi.org/10.17073/1997-308X-2020-75-86>
Князева Ж.В., Юдин П.Е., Петров С.С., Максимук А.В. Применение металлизационных покрытий для защиты погружных электродвигателей насосного оборудования от воздействия осложняющих факторов в нефтя-
- ных скважинах. *Известия вузов. Порошковая металлургия и функциональные покрытия*. 2020;(1):75–86. <https://doi.org/10.17073/1997-308X-2020-75-86>
7. Li H., Chen G., Zhang G., Zhang K., Luo G. Characteristics of the interface of a laser-quenched steel substrate and chromium electroplate. *Surface and Coatings Technology*. 2006;201:902–907. <https://doi.org/10.1016/j.surfcoat.2006.01.011>
8. Babu B.R., Bhanu S.U., Meera K.S. Waste minimization in electroplating industries: A review. *Journal of Environmental Science and Health. Part C*. 2009;27(3):155–177. <https://doi.org/10.1080/10590500903124158>
9. Malyshev V.V., Shakhnin D.B. Titanium coating on carbon steel: direct-current and impulsive electrodeposition. Physicomechanical and chemical properties. *Materials Science*. 2014;50(1):80–91. <https://doi.org/10.1007/s11003-014-9694-7>
10. Ramezani-Varzaneh H.A., Allahkaram S.R., Isakhani-Zakaria M. Effects of phosphorus content on corrosion behavior of trivalent chromium coatings in 3.5 wt.% NaCl solution. *Surface and Coatings Technology*. 2014;244:158–165. <https://doi.org/10.3390/coatings9090531>
11. Bahrami A., Delgado A., Onofre C., Muhl S., Rodil S.E. Structure, mechanical properties and corrosion resistance of amorphous Ti–Cr–O coatings. *Surface and Coatings Technology*. 2019;374:690–699. <https://doi.org/10.1016/j.surfcoat.2019.06.061>
12. Trigodet F., Larché N., Morrison H.G., Maignien L., Thierry D. Influence of dissolved oxygen content on the bacteria-induced ennoblement of stainless steels in seawater and its consequence on the localized corrosion risk. *Materials and Corrosion*. 2019;70(12):2238–2246. <https://doi.org/10.1002/maco.201911225>
13. Zhang E., Li S., Ren J., Zhang L., Han Y. Effect of extrusion processing on the microstructure, mechanical properties, biocorrosion properties and antibacterial properties of Ti–Cu sintered alloys. *Materials Science and Engineering: C*. 2016; 69:760–768. <https://doi.org/10.1016/j.msec.2016.07.051>
14. Burkov A.A., Chigrin P.G. Effect of tungsten, molybdenum, nickel and cobalt on the corrosion and wear performance of Fe-based metallic glass coatings. *Surface and Coatings Technology*. 2018;351:68–77. <https://doi.org/10.1016/j.surfcoat.2018.07.078>
15. Burkov A.A., Krutikova V.O. Deposition of amorphous hardening coatings by electrospark treatment in a crystalline granule mixture. *Powder Metallurgy and Functional Coatings*. 2019;(2):57–67. (In Russ.). <https://doi.org/10.17073/1997-308X-2019-2-57-67>
Бурков А.А., Крутикова В.О. Осаждение аморфных упрочняющих покрытий электроискровой обработкой в смеси кристаллических гранул. *Известия вузов. Порошковая металлургия и функциональные покрытия*. 2019;(2):57–67. <https://doi.org/10.17073/1997-308X-2019-2-57-67>
16. Burkov A.A., Kulik M.A. Wear-resistant and anticorrosive coatings based on chrome carbide Cr₇C₃ obtained by electric spark deposition. *Protection of Metals and Physical Chemistry of Surfaces*. 2020;56(6):1217–1221. <https://doi.org/10.1134/S2070205120060064>

17. Cao G., Zhang X., Tang G., Ma X. Microstructure and corrosion behavior of Cr coating on M50 steel fabricated by electrospark deposition. *Journal of Materials Engineering and Performance*. 2019;28(7):4086–4094. <https://doi.org/10.1007/s11665-019-04148-2>
18. Li Y.C., Zhang W.W., Wang Y., Zhang X.Y., Sun L.L. Effect of spray powder particle size on the bionic hydrophobic structures and corrosion performance of Fe-based amorphous metallic coatings. *Surface and Coatings Technology*. 2022;437:128377. <https://doi.org/10.1016/j.surfcoat.2022.128377>
19. Wang Q.Y., Xi Y.C., Zhao Y.H., Liu S., Bai S.L., Liu Z.D. Effects of laser re-melting and annealing on microstructure, mechanical property and corrosion resistance of Fe-based amorphous/crystalline composite coating. *Materials Characterization*. 2017;127:239–247. <https://doi.org/10.1016/j.matchar.2017.03.011>
20. Shafyei H., Salehi M., Bahrami A. Fabrication, microstructural characterization and mechanical properties evaluation of Ti/TiB/TiB₂ composite coatings deposited on Ti6Al4V alloy by electro-spark deposition method. *Ceramics International*. 2020;46(10): 15276–15284. <https://doi.org/10.1016/j.ceramint.2020.03.068>
21. Yu J., Liu Y., Song B., Wang J. Microstructure and properties of Fe-based alloy coating on gray cast iron fabricated using induction cladding. *Coatings*. 2020; 10(9):801. <https://doi.org/10.3390/coatings10090801>

Information about the Authors




Сведения об авторах

Aleksandr A. Burkov – Cand. Sci. (Phys.-Math.), Senior Researcher, Head of the Laboratory of Physical and Chemical Fundamentals of Materials and Technology, Institute of Materials Science of the Khabarovsk Federal Research Center of the Far Eastern Branch of the Russian Academy of Sciences

 **ORCID:** 0000-0002-5636-4669

 **E-mail:** burkovalex@mail.ru

Mariya A. Kulik – Junior Researcher of the Laboratory of Physical and Chemical Fundamentals of Materials and Technology, Institute of Materials Science of the Khabarovsk Federal Research Center of the Far Eastern Branch of the Russian Academy of Sciences

 **ORCID:** 0000-0002-4857-1887


 **E-mail:** marijka80@mail.ru

Александр Анатольевич Бурков – к.ф.-м.н., ст. науч. сотрудник, заведующий лабораторией физико-химических основ технологии материалов, Институт материаловедения Хабаровского федерального исследовательского центра Дальневосточного отделения РАН

 **ORCID:** 0000-0002-5636-4669

 **E-mail:** burkovalex@mail.ru

Мария Андреевна Кулик – мл. науч. сотрудник лаборатории физико-химических основ технологии материалов, Институт материаловедения Хабаровского федерального исследовательского центра Дальневосточного отделения РАН

 **ORCID:** 0000-0002-4857-1887

 **E-mail:** marijka80@mail.ru

Contribution of the Authors



Вклад авторов

A. A. Burkov – formulated the concept of the article, reviewed publications, conducted experiments, processed and analyzed data, wrote the manuscript, and edited the text.

M. A. Kulik – studied the microhardness and structure of samples, searched for and analyzed published data, and contributed to manuscript design.

А. А. Бурков – идея статьи, литературный обзор, проведение экспериментов, обработка и анализ данных, подготовка текста.

М. А. Кулик – исследование микротвердости и структуры образцов, поиск и анализ литературных данных, редактирование текста, оформление статьи.

Received 21.12.2022

Revised 30.12.2022

Accepted 13.01.2023

Статья поступила 21.12.2022 г.

Доработана 30.12.2022 г.

Принята к публикации 13.01.2023 г.